DUST SILICATE EMISSION IN FIR/SUBMM

A. Coupeaud[1], K. Demyk[1], C. Mény[1] and C. Nayral[2]

Abstract. The far-infrared to millimeter wavelength (FIR-mm) range in astronomical observations is dominated by the thermal emission from large (10-100 nm) and cold (10-20 K) dust grains, which are in thermal equilibrium with the interstellar radiation field. However, the physics of the FIR-mm emission from such cold matter is not well understood as shown by the observed dependence with the temperature of the spectral index of the dust emissivity β and by the observed far infrared excess. Interestingly, a similar behaviour is observed in experiments of characterization of the spectral properties of dust analogues. We present a study of the optical properties of analogues of interstellar silicate grains at low temperature in the FIR/submm range aiming to understand their peculiar behaviour. Such studies are essential for the interpretation of the Herschel and Planck data.

Keywords: analogues interstellar grains, emissivity spectral index, temperature, anticorrelation, submillimeter wavelength range, Herschel, Planck

1   Introduction

The Interstellar Medium (ISM) is composed of 99 % of gas and 1 % of dust. Interstellar dust has the property to absorb and scatter UV-visible photons produced by stars and is thus the dominant source of opacity in our galaxy. Among the three major components invoked in the model of Désert et al. (1990), the big grains are large enough (10-100 nm) to be at the thermal equilibrium with the interstellar radiation field, at temperatures of a few tens of K and thus emit in the far infrared (FIR). An important component of these grains is silicates. They explain in particular the bands observed at 9.7 and 18 μm and are predominantly in the amorphous state in the ISM. Thanks to ISO and the discovery of emission bands from crystallized silicate in various environments, we now know that these silicates are mostly magnesium and iron rich silicates such as pyroxene ($Mg_xFe_{1-x}SiO_3$) and olivine ($Mg_xFe_{2-2x}SiO_4$). These silicate grains dominate the dust emission in the far-infrared/submillimeter range which is usually expressed as follow: $I_\lambda = M_d \kappa_{\lambda_0} (\frac{\lambda}{\lambda_0})^{-\beta} B_\lambda(T)$, where I_λ is the spectral intensity, $B_\lambda(T)$ is the Planck function at the dust temperature, M_d is the column density of grains along the line of sight, κ is the mass absorption coefficient and β is the emissivity spectral index. Simple semi-classical models of absorption, such as the Lorentz model for damping oscillators and the Drude model for free charge carriers, provide a temperature independent asymptotic value $\beta=2$ for 3D solids. However, this value of the spectral index is not in agreement with the observations of the FIR/submm SED of interstellar dust emission (Dupac et al. 2003; Désert et al. 2008; Reach et al. 1995).

Indeed, over various sites of the ISM, PRONAOS observations revealed an anticorrelation between the dust grain mean temperature T and the emissivity spectral index β, with β values go down to $\sim$ 1 at 80 K and up to 2.4 at 11 K (Dupac et al. 2003). Désert et al. (2008) confirmed this inverse relationship found by PRONAOS, with β values decrease to 1.3 at 25 K and increase to 4 below 10 K. In addition, the data of the FIRAS instrument on board the COBE (Cosmic Background Explorer) satellite revealed the existence of a significant millimeter excess of the dust emission with respect to a single greybody law. This has been interpreted as due to the presence of very cold dust (5-7 K) in the ISM (Finkbeiner et al. 1999) in addition to a warmer component responsible for the emission maximum near 100 μm. However, the millimeter excess appeared to be extremely

[1] Université de Toulouse, UPS, CESR, 9 avenue du colonel Roche, F-31028 Toulouse cedex 4, France and CNRS, UMR5187, F-31028 Toulouse, France

[2] Université de Toulouse, INSA, UPS, LPCNO, 135 avenue de Rangueil, F-31077 Toulouse France and CNRS, LPCNO, F-31077 Toulouse France

well correlated with the FIR dust emission. This could be indicative of a situation in which the excess could also be produced by unidentified processes intrinsic to the grain component radiating at thermal equilibrium, without requiring an additional colder component. The first results of the Herschel mission show the observed submm excess previously observed by Reach et al. (1995) in many different sources in our Galaxy (Anderson et al. 2010; Rodon et al. 2010) and in external galaxies such as the Magellanic Clouds (Bot et al. 2010).

At the same time, different laboratory studies of the spectral properties of astronomical dust analogues in the FIR/submm spectral range at low temperature have been performed. Agladze et al. (1996) found that the absorption coefficient of $2MgO.SiO_2$ and $MgO.2SiO_2$ grains decreases with increasing temperature up to 20 K and then increases again at higher temperature in the $700\mu m$-3mm range. Mennella et al. (1998) reported a significant temperature dependence of the emissivity spectral index for the amorphous iron rich silicate $FeSiO_4$ (β =2.1 at 24 K down to 1.4 at 294 K) in the $200\mu m$-2mm range. Boudet et al. (2005) performed measurements on different types of amorphous silicates as $MgSiO_3$ for temperature between 10 and 300 K and wavelengths from 100 μm to 1mm. They confirmed a strong temperature and frequency dependency of the absorption coefficient.

Despite all these observational and experimental evidence, the phenomenological origin of this β-T anticorrelation remains unclear. More experimental studies are required in order to progress in the understanding of the physical and chemical grain properties responsible for the temperature-dependent optical behavior observed in the ISM. It appears crucial to perform new measurements on other amorphous materials in a more extended wavelength range for the data analysis of the Herschel and Planck missions.

2 Experiments

A better understanding of optical properties does not necessarily require working on realistic interstellar analogues; one way is to work first on the expected simplest solids showing these properties. We have thus chosen to study silica, SiO_2 and three amorphous Mg-rich silicates which are classical astronomical dust analogues: one olivine-type Mg_2SiO_4 and two pyroxenes-type $MgSiO_3$ and $CaMgSi_2O_6$. The silica samples were synthesised with a sol-gel method, according to the published procedure (El Hawi et al. 2009), which allow us to control some essential parameters like the size, the morphology and the porosity of the nanoparticles. These parameters are characterized by Transmission Electronic Microscopy (TEM) to measure the size and specify the shape of the nanoparticles; by X Rays Diffraction (XRD) to define if the material is amorphous or crystalline and by Nuclear Magnetic Resonance (NMR) to characterize the environment around the silicon and hydrogen atoms in the material. This last method is very important because of the hydrophilic character of the silica which leads to water adsorption and silanols (SiOH groups) formation. This hydrophilic character depends on the state of the surface and on the synthesis process (dry or wet processes) and thus varies from sample to sample. We have studied different amorphous silica samples having different size, synthesis method, water and SiOH content, porosity. We synthesised spheroidal and non porous SiO_2 nanoparticles of 37±14 nm and 154±30 nm diameter, a specific area about 30±15 m^2/g and a density of $\sim$ 1.7±15 g/cm^3. Commercially SiO_2 samples consist of non porous spherical particles with 500 nm diameter (Lancaster) and silica-fumed agglomerates (Aldrich). The silica fumed is composed of 7 nm spherical particles linked together to form micrometer chains, very highly branched with a high surface area (390±40 m^2/g). The silicate were synthesised by sol-gel method according to the procedures described in Mitchell et al. (1998) and Gillot et al. (2009). To remove the organic residual from the synthesis, all the silicate samples were heated up to 400°C or 500°C depending on the synthesis procedure. TEM characterization shows that the grains are micrometer-sized grains for the Mg_2SiO_4 sample and have an average grains size of $\sim$100 nm for the $MgSiO_3$ and $CaMgSi_2O_6$ samples. These silicates presented specific area comprised between 80 and 130 m^2/g.

For the FIR spectroscopic measurements all these silica and silicate powder samples were mixed with polyethylene powder at 120°C and we applied on this homogeneous mixture a pressure of 7 tons during 5 min to obtained 10 mm diameter pellets. The FIR/submm optical properties of the samples were measured with the experimental set-up ESPOIRS. It is composed of a spectrometer Bruker IFS113V Fourier Transform InfraRed (FTIR) coupled with a cryostat which allows us to cool down our samples from 300 K to 4 K. The spectrometer is equipped with a Hg lamp source, different Mylar beam splitters with thickness of 3.5, 12, 23, 50, 100 μm and a 4 K-bolometer detector. This configuration allows to perform measurements in the 2 - 800 μm wavelength range (5000 - 12.5 cm^{-1}). The transmittance spectra were calculated by dividing the spectrum of the sample pellet by the one of a blank polyethylene pellet. The transmission spectra of each sample were recorded during a cooling cycle from room temperature (300 K) to 10 K. To complete our wavelength range from 800 to 1000 μm

we performed some experiments on the AILES (Advanced Infrared Line Exploited for Spectroscopy) beamline at the synchrotron SOLEIL (Brubach et al. 2010). The mass absorption coefficient of the measured sample is derived from the transmission spectrum according to : $\kappa = \kappa_{\lambda_0} \ (\lambda/\lambda_0)^{-\beta}$

3   Results : evolution of the optical properties

The complete study about the four silica samples is detailed in Coupeaud et al. (in preparation). We only discuss here the results for the silica fumed and the 30 nm silica samples (Fig. 1. a) and b)). First, we observe for both samples the decrease of κ with decreasing temperature. This decrease of opacity with temperature is greatly enhanced for long wavelengths. Furthermore, we report a break in the absorption curves around 350 μm especially obvious for silica sample of 30 nm. The spectral index, measured between 350 and 600 μm, increases when the temperature decreases for both silica samples: $\beta \sim 1$ and $\beta \sim 2$ at 300 K, $\beta \sim 2$; $\beta \sim 3$ at 10 K, for the fumed and the 30 nm silica samples, respectively. We thus observe experimentally an anticorrelation β-T. Similar results are found for all the four silica samples (Coupeaud et al., in preparation).
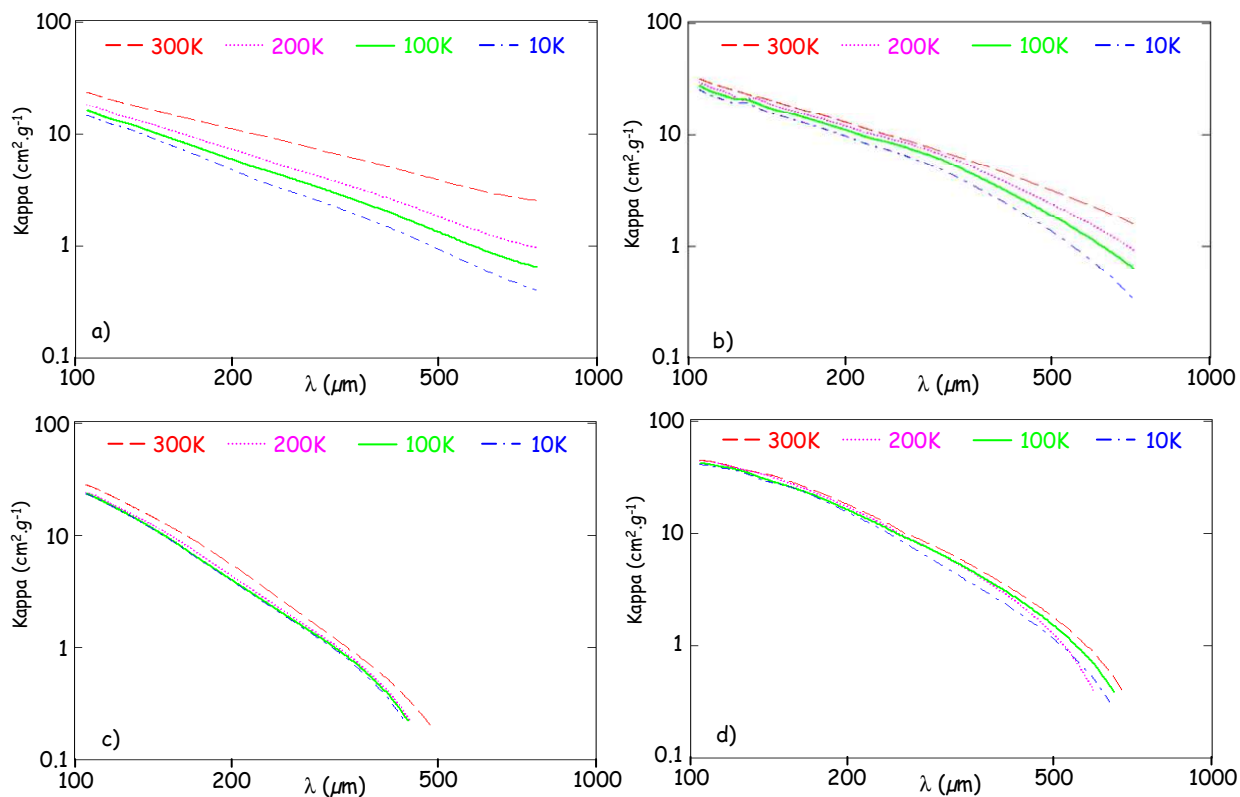

Fig. 1. Evolution of the mass absorption coefficient κ $(cm^2\,g^{-1})$ as a function of the wavelength λ (μm) at 300 K, 200 K, 100 K and 10 K for a) the amorphous (non annealed) silica fumed, b) the amorphous (non annealed) silica 30 nm diameter, c) the crystalline (annealed at 1300°C) silica fumed and d) the crystalline (annealed at 1100°C) silica 30 nm diameter.

To investigate the hypothesis that OH groups present in silica are responsible for the anticorrelation, the silica powders were heated at different temperatures. Indeed, a thermal treatment at the appropriate temperature leads to the dehydration (the removal of physically adsorbed water) and dehydroxylation (the removal of silanol groups from the silica surface). Annealing at 200°C remove physisorbed water (Serp et al. 2002; Ek et al. 2001) while the dehydroxylation processes occur slowly from 200°C up to 1200°C. The temperatures at which physisorbed water and silanol groups were assumed to be totally released were dependent on the silica (Zhuravlev 2000; Ek et al. 2001). For the crystallized silica fumed and 30nm silica samples, we observe no variation of κ and β with the temperature (Fig. 1. c) and d)) and these observations are the same for the four silica samples. This shows that the β-T anticorrelation observed is related to the defects in the amorphous structure of the material (eg. SiOH content). For more details see Coupeaud et al. (in preparation).

Then, we report the evolution of κ as a function of λ in logarithmic scale at different temperatures for the amorphous and crystallized Mg_2SiO_4 sample (Fig. 2. a) and b)). For the amorphous sample, as for silica, κ decreases with decreasing temperature and this decrease of opacity with the temperature is more pronounced at long wavelengths. Furthermore, we report a break around 650 μm especially obvious for low temperatures $\leq$ 100 K. The spectral index measured between 650 and 1000 μm is equal to $\beta \sim 2.6$ at 300 K, it increases to $\beta \sim 4$ at 10 K. Unlike silica, the OH content cannot be responsible for this behaviour because of the thermal treatment at 500 °C which eliminates the silanol groups in this silicate sample. In this case, the defects involved could be created by the Mg^{2+} ions present in the material. To test this hypothesis, we have annealed the samples until the crystallization of forsterite. We observe no variation of κ and β with temperature for the cristallized sample(Fig. 2. b)). This indicates that the β-T anticorrelation observed is related to the defects in the amorphous structure of the material (eg. Mg^{2+} ions content, porosity). For more details see Coupeaud et al. (in preparation).
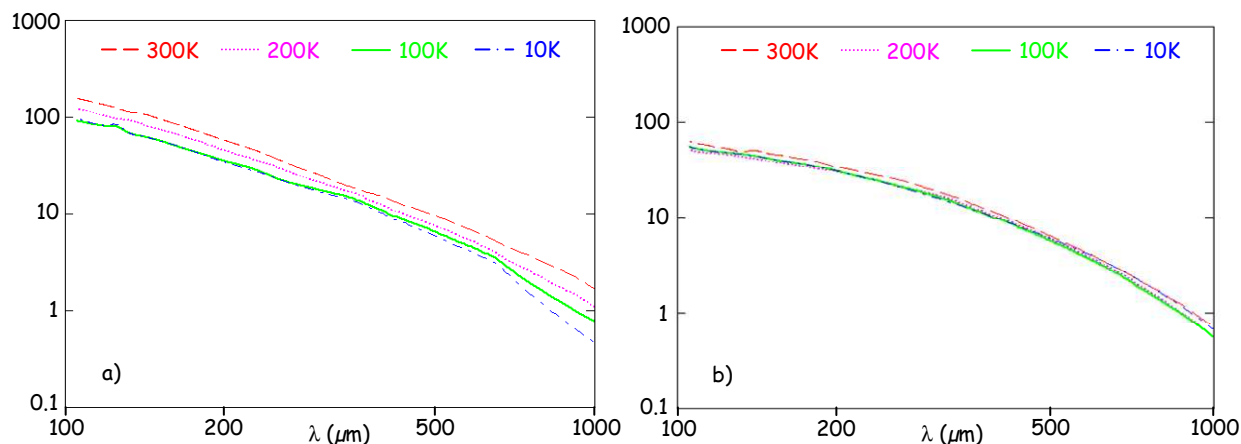

Fig. 2. Evolution of the mass absorption coefficient κ $(cm^2 \, g^{-1})$ as a function of the wavelength λ (μm) at 300 K, 200 K, 100 K and 10 K for a) the amorphous (annealed at 500°C) Mg_2SiO_4 and b) the crystalline (annealed at 1100 °C) forsterite

4   Conclusions

In all amorphous samples, the absorption shows an anticorrelation between the temperature and the spectral index, in qualitative agreement with astrophysical data. The temperature dependent absorption is related to the amorphous state of the material. It can be modified with various annealing of the amorphous sample, and suppressed when annealing leads to crystallization of the samples. In the amorphous materials and at a given temperature, the spectral index cannot anymore be considered as a constant over the whole submillimeter spectral range. This, and the decrease of the opacity with the temperature must be taken into account for the analysis of Herschel/Planck data.

References

Agladze, N. I., Sievers, A. J., Jones, S. A., Burlitch, J. M., & Beckwith, S. V. W. 1996, ApJ., 462, 1026

Anderson L.D, Zavagno, A., Rodon, J., et al. 2010, A&A 518, L99

Bot, C., Ysard, N., Paradis, D., et al. accepted in A&A

Boudet, N., Mutschke, H., Nayral, C., et al. 2005, ApJ., 633, 272

Brubach, J.B., Manceron, L., Rouzière, M., et al. 2010, AIP Conference Proceedings, 1214, 81

Désert, F.-X., Boulanger, F., & Puget, J. L. 1990, A&A, 237, 215

Désert F.-X., Macías-Pérez J. F., Mayet F., et al. 2008, A&A, 481, 411

Dupac, X., Bernard, J.-P., Boudet, N., et al. 2003, A&A, 404, L11

Ek, S., Root, A., Peussa, M., & Niinisto, L. 2001, Thermochimica Acta, 379, 201

El Hawi, N., Nayral, C., Delpech, F., et al. 2009, Langmuir, 25, 7540

Finkbeiner, D.P., Davis, M., & Schlegel, D.J., 1999, ApJ., 524, 867

Gillot, J., Roskosz, M., Depecker, C., Roussel, P., & Leroux, H. 2009, 40th Lunar and Planetary Science Conference, 1763

Mennella, V., Brucato, J. R., Colangeli, L., et al. 1998, ApJ., 462, 1026

Mitchell, M.B.D., Jackson, D., & James, P.F. 1998, J. of Sol-Gel Science and Technology, 13, 359

Reach, W. T., Dwek, E., Fixsen, D. J., et al. 1995, ApJ., 451, 188

Rodon, J.A., Zavagno, A., Baluteau, j,-P., et al. 2010, A&A 518, L80

Serp, P., Kalck, P., & Feurer, R. 2002, Chem. Rev., 102, 3085

Zhuravlev, L.T. 2000, Colloids and Surfaces A, 173, 1